Simulating Poloidal Impurity Density Variation in the Tokamak Pedestal

Liam Carpenter

New York University, Courant Institute of Mathematical Sciences
Email: lc3919@nyu.edu

Nuclear Fusion is one of the most promising forms of practical energy production for the 21st century. By simulating the physics of the sun on earth we have the potential to produce nearly unlimited clean and cheap energy. To this point, our current understanding of the physics happening inside the state of the art fusion reactors is limited, with theoretical predictions about physical behavior in the outer edge regions of the plasma not lining up with experimental findings. In this paper we verify one aspect of a new theoretical model, that of impurity behavior, for the edge physics of a tokamak fusion reactor. For the first time the radial and diamagnetic flow effects between nested flux surfaces is included in the model. In solving the newly derived ordinary differential equation using fixed point iteration and Fourier pseudospectral methods we achieve results in line with experimental predictions of the impurity behavior in the tokamak edge region. This opens the door to better understanding of the impurity and fueling processes of modern fusion reactors and will hopefully allow for more efficient reactor design and accurate simulations in the future.

1. INTRODUCTION

Modern day fusion reactors are still not at the point of being realistically usable. The most state of the art project, the ITER (International Thermonuclear Experimental Reactor), is promised to finally reach break even production in 2026. One of the major efficiency problems in these fusion reactors comes from the problem of confining the super hot plasma in the first place. To do this, high atomic number, known as high-z, materials are used. These high-z materials bleed impurities into the plasma and, through radiative losses, reduce the efficiency of the plasma Espinosa[5]. To this points, understanding the way these impurities behave is useful for the design and simulation of fusion reactors. The behavior of impurities in the core of the plasma is well understood, but the edge region of the plasma, known as the pedestal, presents complications. In the pedestal region, plasma density drops off quickly giving inspiration for the name of the region from the characteristic "pedestal" like curve shown in bottom plot of figure 1 Previous theoretical models for the impurity dynamics in this region ignore the effects impurity flow between flux surfaces. In ignoring these effects the model under-predicts the experimental in-board over out-board impurity density ratio Helander[1]. This indicates that previous theories are missing some critical phenomena. Espinosa 2018, constructed a model which retained these radial effects. In this paper we solve the ordinary differential equation derived in the aforementioned paper that includes radial and diamagnetic flow effect. In doing so we aim to confirm that the radial and diamagnetic effects are amplifying the asymmetry driven by the magnetic field,

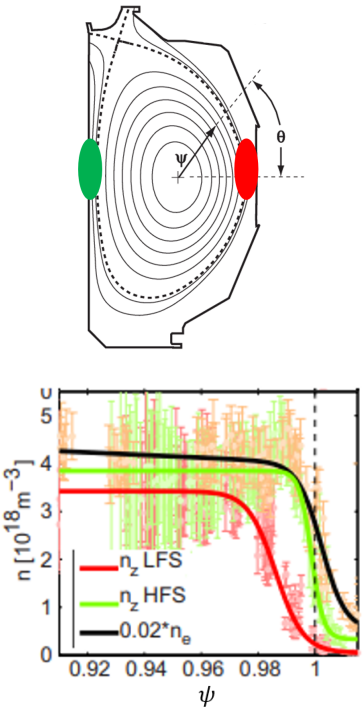

FIGURE 1. Radial impurity density profiles from Alcator C-mod reactor, adapted from Churchill[4] and tokamak cross section with coloring matching density profile data adapted from Evans[3]

thus opening the door to better future design and simulation of these reactors.

2. MODEL AND COMPUTATIONS

2.1. Mathematical Model and Notation

The model we are looking to solve takes the form of a non-linear ordinary differential equation.

$$\alpha n\frac{\partial n}{\partial \theta} + (g + U + \alpha D) + (b^2 - 1)(g - D) = -\frac{\partial n}{\partial \theta} + n(g + U + \alpha D) \tag{1}$$

First we have the experimentally derived terms. Which we treat as constants in the equation.

- α: Effective Impurity Charge
- g: Bulk Ion Diamagnetic Friction
- U: Kinetic
- D: Impurity Diamagnetic Friction

Of particular note here is the D term. When $D = 0$ the previous model by Helander is recovered. Then we have our functions of theta, the poloidal angle variable.

- n: Impurity Density (Unknown)
- b^2: Dimensionless Magnetic Field Squared

$$b^2 = 1 - \frac{1}{3}\cos(\theta)$$

Here we are using a single cosinusoidal approximation of the magnetic field. The linearized version of this ordinary differential equation is given by,

$$(1+\alpha)\frac{\partial n}{\partial \theta} = (n-1)(g+U+\alpha D) + (1-b^2)(g-D) \tag{2}$$

The linearized verision of this ODE will be solved as the initial step in our fixed point iteration scheme. We start with the problem set up and the question of how to represent differentiation in the discretized setting.

2.2. Problem Set Up

We begin the setup of this problem by discretizing the domain, which is periodic, ie. $\theta \in [0, 2\pi]$. This gives us a uniform grid of N points such that

$$\theta_0 = 0, \theta_1 = 0 + \Delta x, \ldots, \theta_{n-1} = 2\pi - \Delta x$$

Where Δx is the grid spacing. Then we would like to turn our ODE into a system of N ODE's for each grid point theta. The problem here is representing the differentiation operation. To do this we will use an approach using pseudo-spectral methods, specifically a fourier differentiation matrix as outlined in chapter 3 of Trefethen[2]. To do this we need an interpolating function of the impurity density at the grid points. That is we want a function $p(x)$ such that, $p(x_j) = n_j, \forall j$ The inverse Discrete Fourier Transform will give us one if we evaluate it for all $x \in [\frac{\pi}{\Delta x}, \frac{\pi}{\Delta x}]$. That is our interpolant p will take the form,

$$p(x) = \frac{1}{2\pi}\sum_{k=-N/2}^{N/2} e^{ikx}\hat{n_k} \tag{3}$$

All that is left is to find out $\hat{n}$. To represent n at the grid points we will use a linear combination of n at each grid point with a translated delta function,

$$\delta(k-j) = \begin{cases} 1 & j = k \\ 0 & j \neq k \end{cases}$$

We then represent each grid point n_k as,

$$n_k = \sum_{j=0}^{N-1} n_j \delta(k-j) \tag{4}$$

The delta function here, in effect, acts as a sieve and selects only the n that we want but represents it as a global sum of all the n's. Since the n_j's here are just constants, they can be factored out of the initial Fourier transform. We are then left with determining the Fourier transform of the translated delta function. This is a well known Fourier transform and gives the grid size Δx. The inverse DFT then can be applied in the same way. A summation by parts yields the translated periodic Sinc function as the inverse Fourier transform of the grid size.

$$S_N(x - x_k) = \frac{\sin(\frac{\pi x - x_k}{\Delta x})}{\frac{2\pi}{\Delta x}\tan(\frac{x-x_k}{2})}$$

This is the unique L^2 band limited interpolant of the translated delta function. L^2 being the set of functions such that the square of the absolute value has a finite integral over the entire real line. So we have,

$$S_N(x - x_k) = \begin{cases} 1 & x = x_k \\ 0 & x = x_j, j \neq k \end{cases} \tag{5}$$

With this in mind from (3) we see our interpolating function $p(x)$ will be

$$p(x) = \sum_{j=0}^{N-1} n_j S_N(x - x_k), \quad x \in [\frac{-\pi}{\Delta x}, \frac{\pi}{\Delta x}] \tag{6}$$

So we have taken a discrete representation of our function values and using an interpolating function and the Discrete Fourier Transform and Inverse Discrete Fourier Transform, converted it into a continuous-differentiable function. This interpolating function has a convenient matrix vector representation,

$$\begin{pmatrix} S_N(x_0 - x_0) & \ldots & S_N(x_0 - x_{N-1}) \\ \vdots & \ddots & \vdots \\ S_N(x_0 - x_{N-1}) & \ldots & S_N(x_{N-1} - x_{N-1}) \end{pmatrix} \begin{pmatrix} n_0 \\ \vdots \\ n_{N-1} \end{pmatrix} \tag{7}$$

By differentiating our matrix of periodic Sinc functions at the grid points we can derive our differentiation matrix. The entries of this matrix are found to be

$$(\mathbf{D}^{(1)})_{ij} = \begin{cases} 0 & i = j \\ \frac{1}{2}(-1)^{i+j}\cot(\frac{x_j - x_i}{2}) & i \neq j \end{cases} \quad (8)$$

In constructing our linear system then we will represent the differentiation operator $\frac{d}{d\theta}$ using the differentiation matrix.

2.3. Numerics

Now that we know how to represent the differentiation process, we need to solve the actual ODE. To do this we will implement an iterative procedure based on first solving the linearized ODE, and then using this first vector of n's as a starting point for our non-linear terms. Since we represent the unknown non-linear variables using known numbers from the previous iteration, the non-linear ODE becomes a linear one, which can be solved through the same matrix inversion procedure. The algorithm is as follows

Algorithm 1 Solve Non-Linear ODE

$\mathbf{A} \leftarrow -\mathbf{D}^{(1)} + (g + U + \alpha D)$
$\mathbf{c} \leftarrow (g + U + \alpha D) + (\mathbf{b}^2 - 1)(g - D)$
$\mathbf{n} = \mathbf{A^{-1}c}$
$\mathbf{n}_{old} \leftarrow \mathbf{n}$
$\mathbf{c} \leftarrow \alpha \mathbf{n}_{old}\mathbf{D}^{(1)}\mathbf{n}_{old} + (g + U + \alpha D) + (\mathbf{b}^2 - 1)(g - D)$
$\mathbf{n} = \mathbf{A^{-1}c}$
while $\|\mathbf{n}_{old} - \mathbf{n}\| > threshold$ **do**
  $n_{old} \leftarrow n$
  $\mathbf{c} \leftarrow \alpha \mathbf{n}_{old}\mathbf{D}^{(1)}\mathbf{n}_{old} + (g + U + \alpha D) + (\mathbf{b}^2 - 1)(g - D)$
  $\mathbf{n} = \mathbf{A^{-1}c}$
end while

The first matrix inversion here is equivalent to solving (2).

3. RESULTS

In the experiments that we ran using the above model we were able to achieve the six fold inboard outboard impurity density asymmetry for certain settings of the parameter. Moreover we were able to demonstrate experimentally the increase in impurity density asymmetry with an increase in the diamagnetic friction parameter D. Additionally we compared the results of the linearized version of the ODE, that omitting the $\alpha n \frac{dn}{d\theta}$ term and the full non-linear ODE to show that the results were comparable, though difference were greater in regions with higher impurity density in-out asymmetry. Plot one shows the relationship between the diamagnetic parameter and the impurity density in out symmetry as we increase the Diamagnetic parameter D. The y axis, where $D = 0$ corresponds to the solution to the formulation by Helander[1], where Impurity Diamagnetic Friction is not included. This plot shows how the inclusion of these radial effects magnifies the impurity density in-out asymmetry and even achieves the experimental six-fold value for some representative settings of parameters.

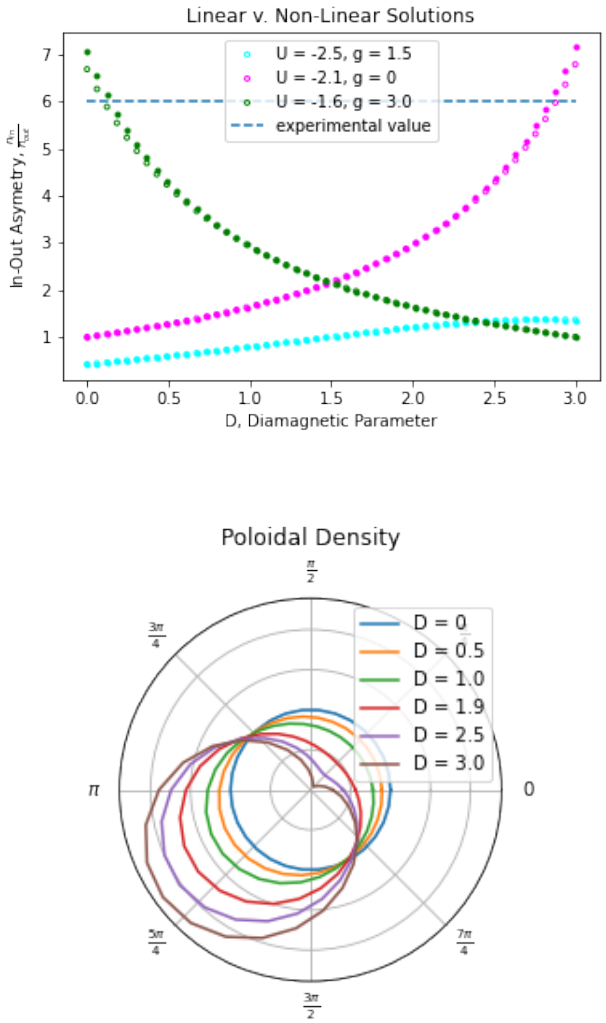

FIGURE 2. Plot one shows a comparison of the impurity density in-out asymmetry between the linear and non-linear with some representative settings of parameters. Plot two shows how the impurities would be distributed for a specific operation mode on a poloidal cross section of the tokamak

The poloidal plot shows the predicted impurity accumulation in more detail. Clearly the impurities tend to accumulate on the inboard, ie. $\theta = \pi$, side of the reactor.

4. CONCLUSION

The results of these numerical simulations confirm that the previous theories for the physics at the tokamak pedestal were missing key factors that become non-negligible when density gradients become steep. The inclusion of these radial effect, those occurring perpendicular to the magnetic fields, are critical to

properly align with experimental findings about the impurity density in-out asymmetry in the tokamak pedestal. While the numerical simulations here where idealized, done using a low order magnetic field expansion and assuming a circular tokamak cross section, they motivate the use of these new terms in future models. The next step in this work is taking the idealized circular cross section and employing a change of coordinates to solve the equation for the actual D shaped tokamak cross section.

REFERENCES

[1] P. Helander. "Bifurcated neoclassical particle transport". In: *Physics of Plasmas* 5 (11 1998). ISSN: 1070664X. DOI: 10.1063/1.873121.

[2] Lloyd N. Trefethen. *Spectral Methods in MATLAB*. 2000. DOI: 10.1137/1.9780898719598.

[3] T E Evans et al. "Experimental signatures of homoclinic tangles in poloidally diverted tokamaks". In: *Journal of Physics: Conference Series* 7 (2005). ISSN: 1742-6588. DOI: 10.1088/1742-6596/7/1/015.

[4] R. M. Churchill et al. "Poloidal asymmetries in edge transport barriers". In: *Physics of Plasmas* 22 (5 2015). ISSN: 10897674. DOI: 10.1063/1.4918353.

[5] Silvia Espinosa and Peter J. Catto. "Theoretical explanation of I-mode impurity removal and energy confinement". In: *Plasma Physics and Controlled Fusion* 60 (9 2018). ISSN: 13616587. DOI: 10.1088/1361-6587/aad0c9.